Synchrotron radiation diffraction study of the mineral moolooite, and synthetic copper oxalates

B. H. O'Connor,[1,a)] R. M. Clarke,[2] and J. A. Kimpton[3]
[1]*Department of Physics and Astronomy, Curtin University, Kent St, Bentley, Perth, WA 6102, Australia*
[2]*ChemCentre, PO Box 1250, Bentley, WA 6983, Australia*
[3]*Australian Synchrotron, 800 Blackburn Road, Clayton, Vic 3168, Australia*

(Received 4 September 2018; accepted 14 January 2019)

The orthorhombic mineral moolooite, CuC_2O_4. nH_2O, described by Clarke and Williams (1986) using Debye-Scherrer photographic data, has a fully-disordered stacking fault (FDSF) structure. Related monoclinic models have been reported for various synthesised samples based on Schmittler (1968). In the present study, synchrotron radiation diffraction data for moolooite and synthesised specimens have been examined with particular reference to crystallographic disorder. The moolooite data correspond to space group *Pnnm*, with $a = 5.3064(2)$, $b = 5.6804(2)$, $c = 2.5630(1)$ Å; $V_c = 77.26(1)$ Å^3; and $Z = 1$; and the FDSF structure along the *b*-direction has been confirmed. The synthetic specimen data from the study indicate partial ordering, with space group $P2_1/n$; and the cell parameters for one specimen being $a = 5.957(7)$, $b = 5.611(5)$, $c = 5.133(7)$ Å; $\beta = 115.16(2)°$; $V_c = 155.27$ Å^3 and $Z = 2$. The level of zeolitic water in the materials has been considered using the approach of Schmittler based on thermogravimetry and pycnometry. The new data for natural topotype material correspond to $CuC_2O_4.1.0H_2O$. It is postulated that the level of water for natural and synthetic specimens may be attributed to the conditions under which the material forms. © *2019 International Centre for Diffraction Data*. [doi:10.1017/S0885715619000101]

Key words: natural moolooite from Mooloo Downs, synthetic moolooite, synchrotron radiation diffraction data, order-disorder structural character, zeolitic water content

I. INTRODUCTION

Papers addressing the structural crystallography for hydrated copper (II) oxalate, CuC_2O_4. nH_2O, extend back over 50 years. Schmittler (1968), in studying a suite of synthetic samples using Guinier X-ray diffraction (XRD), observed sample-to-sample differences involving XRD line shifts, line broadening differences, and the presence of additional lines in some samples. The differences were interpreted in terms of order-disorder (OD) theory (Fichtner-Schmittler, 1979), with the sample-to-sample differences being explained in terms of (i) an orthorhombic, fully-disordered stacking fault (FDSF) structural model (designated the "superposition structure') with space group *Pnnm*; or (ii) an ordered monoclinic structure with space group $P2_1/n$ which was described by Schmittler as "pseudo-orthorhombic'. The space groups, unit-cell parameters and atom coordinates for both models were first proposed by Schmittler (1968). Subsequently, Kondrashev *et al*. (1985) designated the orthorhombic and monoclinic structures as the α- and β-forms, respectively, with the unit cells of the α- and β-forms being related through an orthorhombic-monoclinic transformation. Other papers which have contributed to understanding the structure forms of copper oxalates include Michalowicz *et al*. (1979); Gleizes *et al*. (1980); Fichtner-Schmittler (1984) and Christensen *et al*. (2014). Also relevant is the report of the crystal structure of fully-ordered orthorhombic monohydrate [diaqua-μ-oxalato-copper(II) monohydrate] (Wu and Zhai, 2007)."

A study of natural hydrated copper oxalate material, designated *moolooite by* Clarke and Williams (1986), which had been extracted from mineral specimens collected 12 km from Mooloo Downs Station homestead in Western Australia, described sound fits to Debye-Scherrer XRD data using an orthorhombic cell. Clarke and Williams reported unit-cell dimensions, $a = 5.35$, $b = 5.63$, $c = 2.56$ Å ($V_c = 77.1$ Å^3), after which Chisholm *et al*. (1987) gave very similar values, $a = 5.348$–5.381, $b = 5.625$–5.639, $c = 2.548$–2.559 Å ($V_c = 77.17$ Å^3) for moolooite material extracted from Scandinavian lichens. While the work of Schmittler and others has provided atom coordinates for synthetic material, to date there has been no report of atom coordinates for natural moolooite.

Christensen *et al*. (2014) described the use of laboratory XRD, synchrotron diffraction data (SRD), and neutron diffraction data for synthetic copper oxalate powders to develop a disordered monoclinic $P2_1/n$ structural model for synthetic Cu oxalate specimens, and also provided evidence for there being no crystal water in the structure of the material examined. The structural model has two randomly-occupied Cu and oxalate sites, which are attributed to the existence of anisotropic nano-sized crystallites.

The issue of water content in copper (II) oxalates has not been fully explained. Schmittler (1968) used thermogravimetric analysis and pycnometry to estimate the water content of chemically synthesised oxalate powders and provided plots of unit-cell parameters vs. water content for the a and b

a)Author to whom correspondence should be addressed. Electronic mail: brian_oconnor@iprimus.com.au

unit-cell parameters. Using the Schmittler calibrations, Clarke and Williams reported a moolooite water content corresponding to $n = 0.6$, and Chisholm *et al.* (1987) a range of values $n = 0.4$–0.7 for their lichen moolooite material. This evidence points to there being more take up of water in natural moolooites possibly because the material has been precipitated relatively slowly, compared with synthetics. By contrast, Frost *et al.* (2004) described a thermogravimetric and hot stage Raman study of a reportedly natural moolooite specimen which indicated that the material examined was anhydrous; however, it is noted that the source of the sample was not specified. Taking into account literature reports on the water content issue, it appears that there is no "crystal" water in Cu oxalates, but that zeolitic water may be present depending on the conditions under which the compound forms.

In view of the structural variability, use of the current Powder Diffraction File (PDF) data for copper oxalates (ICDD, 2016) should be viewed with caution. The only indexed pattern for $CuC_2O_4.\ nH_2O$ is PDF 00-021-0297, which derives from Schmittler's data for synthetic samples, and there is no PDF pattern for natural moolooite even though Clarke and Williams had published indexed data for the mineral. Importantly in terms of the current paper, the entry for 00-021-0297 includes the comments *Spacings and intensities vary slightly with n. All data refer to a sample consisting of strongly disordered crystals (stacking disorders in the b-direction; OD structure) and correspond to the periodicity of a superposition structure. Additional reflections owing to ordered crystals may occur … The water content (n between 0 and 1) is a "zeolitic" type.*

The present study was designed to extend the work of Clarke and Williams by examining SRD data for moolooite from Mooloo Downs and also synthetic copper oxalate material with particular reference to defining the crystal structure, including characterising the disordered state of the mineral. An important aspect of the study has been the issue of water content. Additionally, it was intended to clarify confusion from the literature as to the means of identifying natural moolooite and also synthetic copper oxalates using the International Centre for Diffraction Data (ICDD)-PDF data base and pattern simulations, taking into account the complexities of disorder.

II. STRUCTURAL MODELS FOR COPPER OXALATE FROM THE LITERATURE

A. Orthorhombic and monoclinic cells for copper oxalates

Figure 1 shows the relationship between the α-form orthorhombic unit cell for the FDSF structure, following Schmittler (1968) and Kondrashev *et al.* (1985), and the transformed monoclinic cell for the ordered β-form.

The unit-cell parameter transformations are:

$$a_M = a_O/\cos(\beta - 90^\circ)\ldots \quad (1a)$$

$$b_M = b_O\ldots \quad (1b)$$

$$c_M = 2\ xc_O\ldots \quad (1c)$$

$$\beta_M = 90^\circ + \tan^{-1}(c_O/a_O)\ldots \quad (1d)$$

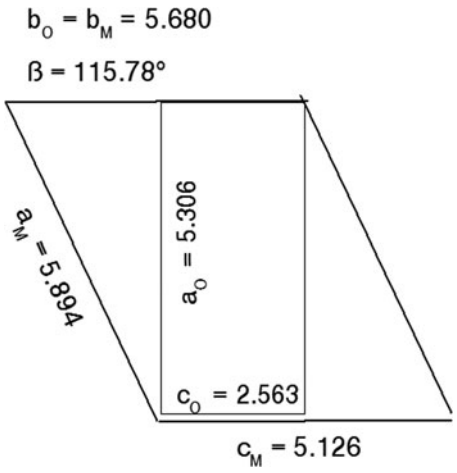

Figure 1. Relationship between the orthorhombic *Pnnm* cell and the alternative monoclinic cell generated by Eqs. 1(a)–(d). Unit-cell parameter values taken from Table IV.

and the relationships between the *hkl* indices for the orthorhombic and monoclinic cells are:

$$h_M = h_O - l_O, k_M = k_O, l_M = 2l_O\ldots \quad (2a)$$

$$h_O = h_M + l_M/2, k_O = k_M, l_O = l_M/2\ldots \quad (2b)$$

Views of the monoclinic model are shown in Figures 2(a) and 2(b), and for the disordered orthorhombic model in Figure 3, respectively.

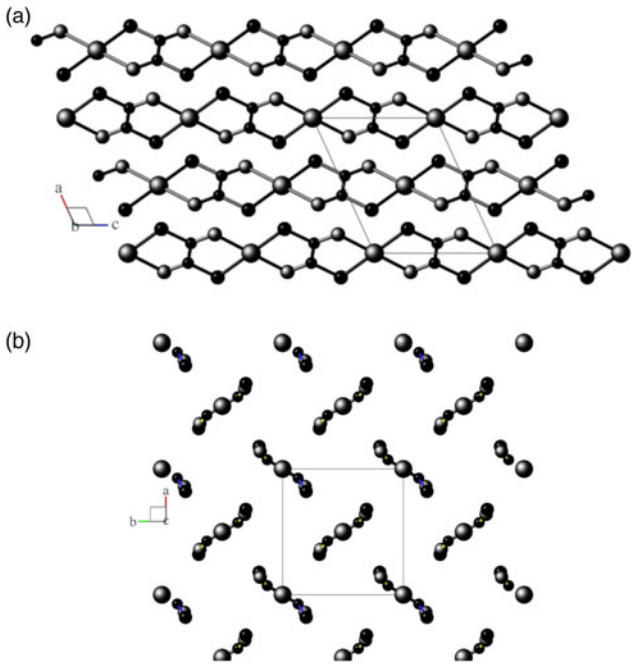

Figure 2. (a) View down the unique *b*-axis of the fully-ordered monoclinic structural model in space group $P2_1/n$, following Kondrashev *et al.* (1985) Atom sizes: Cu = large, O = medium, C = small. Generated using program *Balls & Sticks (V1.80)*. (b) View down the *c*-axis of the fully-ordered monoclinic structural model in space group $P2_1/n$, following Kondrashev *et al.* (1985). See (a) for atom identities.

https://doi.org/10.1017/S0885715619000101 Published online by Cambridge University Press

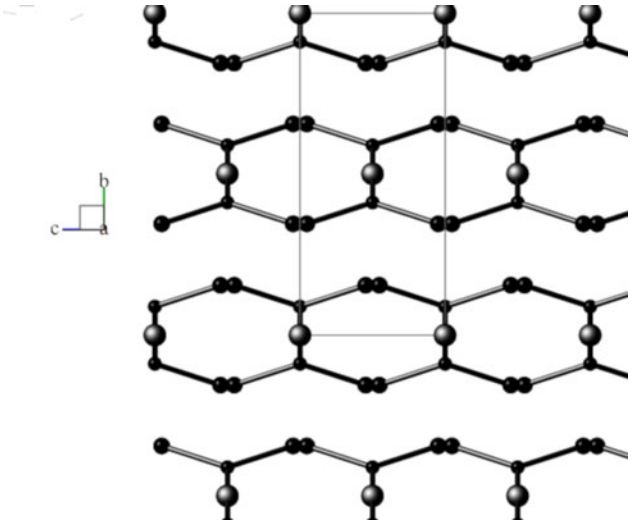

Figure 3. View down the *a*-axis of the FDSF orthorhombic structural model in space group *Pnnm*, following Schmittler (1968, and after RTV optimisation in the current study with SRD data. Atom sizes: Cu = large, O = medium, C = small. Generated using program *Balls & Sticks (V1.80)*.

B. XRD patterns for copper oxalate models from OD theory

Fichtner-Schmittler (1979) summarised the aspects of OD theory which are relevant to copper oxalate crystallography. Key statements from the review are –

(i) Different stackings of OD layers result in ordered structures (periodic in three dimensions) and/or disordered structures, with different stackings possibly occurring in individual crystallites. The various structures which may occur for a particular material are called *polytypes*.

(ii) Any XRD pattern of OD material includes reflections that are common to all members of the respective family: the *family reflections*.

(iii) the family reflections are those for a fictitious structure which is periodic in three dimensions: the *superposition structure*. It is demonstrated in this paper that the natural moolooite material characterised by SRD corresponds to the superposition structure.

(iv) Amongst the ordered structures for any family there is a small number of so-called Maximum Degree of Order (MDO) polytype structures. For Cu oxalate, Fichtner-Schmittler (1979) designated two likely MDO structures as MDO_1 and MDO_2, and provided XRD simulations for each and also for the superposition structure.

Figure 4 shows a comparison of (i) SRD pattern for moolooite from this study and simulated pattern intensities for the superposition structure of Cu oxalate; and (ii) SRD pattern for CSIRO-SYN synthesised Cu oxalate from this study and simulated intensities for the MDO_1 and MDO_2 polytype structures. It is evident by inspection that the natural moolooite SRD pattern agrees closely with the Cu oxalate superposition structure, whereas the SRD pattern for CSIRO-SYN is very similar to that simulated for the MDO_1 polytype.

III. EXPERIMENTAL

A. Materials

The moolooite material for SRD analysis was sourced from Mooloo Downs (Clarke and Williams, 1986), being designated topotype specimen C7 as registered under ChemCentre laboratory number 13F1170 – see Clarke and Williams for a description of the material described previously – physical appearance, microscopy, chemical analysis, and Debye-Scherrer XRD data. In summary, (i) the material is composed of turquoise-green aggregates of generally sub-micron sized equidimensional crystallites; and (ii) from microchemical analysis corresponds to the empirical formula $CuC_2O_4.\ 0.44H_2O$.

Two Cu oxalate samples were chemically synthesised as follows –

(i) Sample CSIRO-SYN was prepared by slowly adding a solution of oxalic acid dihydrate to a solution containing a stoichiometric mass of copper sulphate pentahydrate. The mixture was allowed to stand under ambient laboratory conditions for several hours. The pale blue precipitate was filtered, washed thoroughly with water and air-dried. The SRD pattern showed that a slight excess of the copper salt (*ca*. 3% by weight from Rietveld analysis) was present in the Cu oxalate product.

(ii) Sample GCLSYNF was prepared by the same procedure after substituting an equivalent mass of copper acetate monohydrate for $CuSO_4.5H_2O$. The purity of the precipitate as copper oxalate was confirmed by CHN microanalysis.

B. SRD data measurement and analysis

For SRD analysis, the three samples were manually dispersed by shearing between glass slides to a granularity <<10 μm. Approximately 1 mg of material was mounted for SRD analysis in a 0.2 mm diameter glass capillary. The composite sample of natural moolooite varied in colour from grey near the sealed end of the capillary to turquoise in the central region, with the discolouration being attributed to differences in radiation colour-centre densities following variable exposure to laboratory XRD radiation.

SRD patterns were measured using the Powder Diffraction Beamline at the Australian Synchrotron (AS) which was set to provide a photon energy 18.0068 keV (λ = 0.68816 Å). Each capillary was mounted on a crystallographic goniometer head and rotated at 15 rpm. Patterns were measured using Debye-Scherrer geometry with a goniometer diameter = 152 cm, over the 2θ range 5.5087° to 85.3236° and with an effective step size = 0.00375°. The SRD incident and diffracted beams were fully polarised. The incident beam dimensions at the capillary were approximately 3 mm × 1 mm. Two patterns were measured for the natural moolooite – one for the central 5 mm portion (Pattern A – mainly turquoise material) and a second pattern at the end of the capillary which included grey material (Pattern B). Patterns were measured with a 16 module Mythen II microstrip X-ray detector system (Schmitt *et al*., 2003), each module covering *ca.* 4.8° in 2θ with there being a gap of *ca.* 0.2° between the segments covered by adjacent detector modules. Each pattern was measured twice using 600 s acquisitions, with the Mythen detector

https://doi.org/10.1017/S0885715619000101 Published online by Cambridge University Press

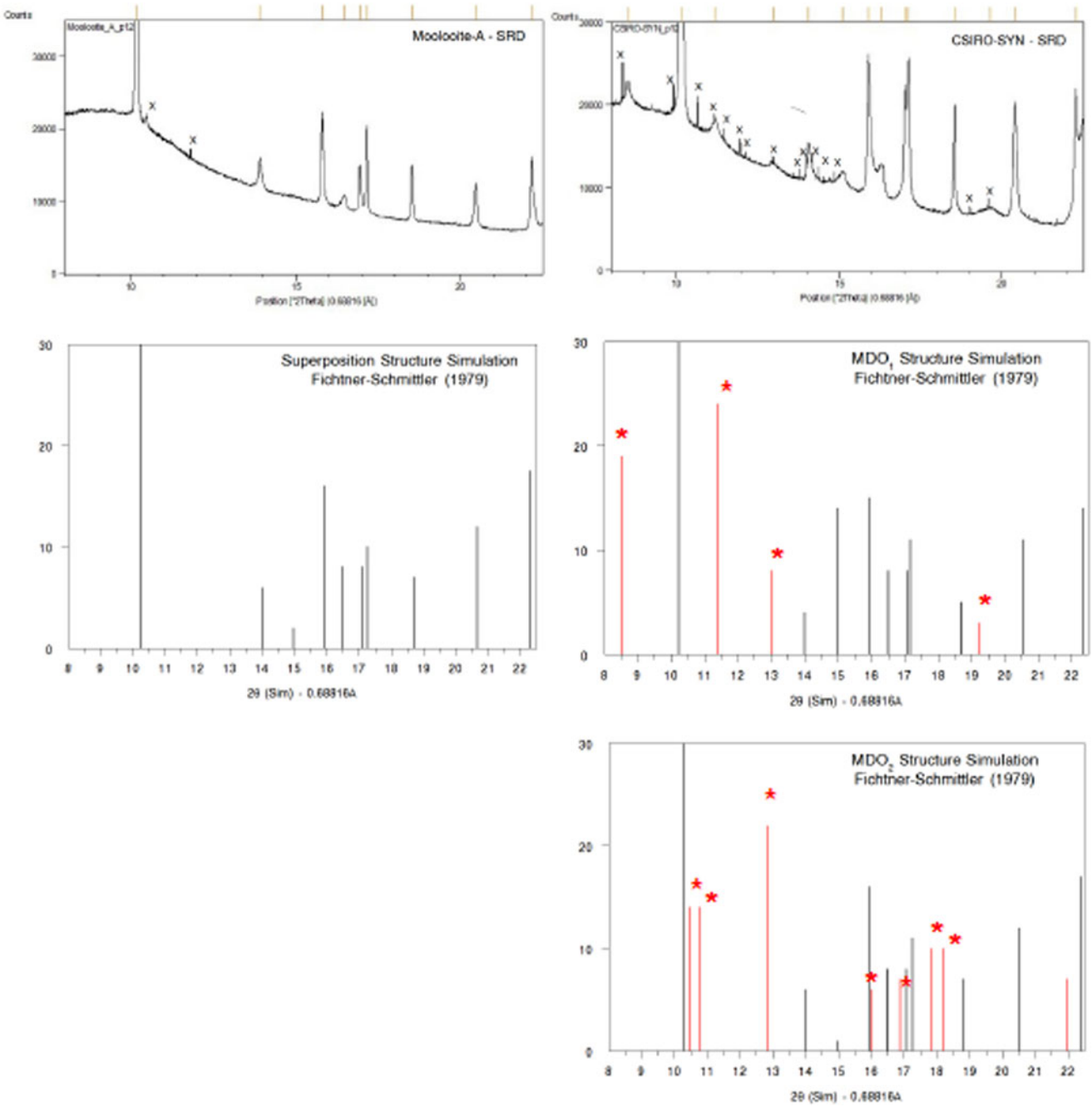

Figure 4. (Color online) Comparison of OD patterns simulated by Fichtner-Schmittler (1979) with the measured SRD patterns. Left diagram pair: simulated pattern for superposition structure compared with natural moolooite SRD pattern: x = contaminant lines for middlebackite and quartz impurities (10.5 and 11.8°, respectively). Right diagram set: simulated patterns for MDO_1 structure (centre) and MDO_2 structure (below) compared with CSIRO-SYN synthetic copper oxalate SRD pattern. The red reflection lines (marked with asterisk) are non-family reflections for the polytype. x = contaminant lines from 3% $CuSO_4$. $5H_2O$ reagent in the measured SRD pattern.

being off-set by 0.5° for the second data acquisition. The two off-set patterns were merged using the program PDViPeR. An additional pattern was measured for a NIST SRM-660b LaB_6 powder under exactly the same conditions to determine the instrument wavelength, the $2\theta_0$ correction and the instrument full-width-half-maximum (FWHM) widths for the Bragg peaks. A $2\theta_0$ value = 0.0036° was determined by Rietveld fitting to the LaB_6 data. Peak positions, above-background intensities and FWHM peak widths were determined with the PANalytical HighScore Plus (HSP) Version 3.0 utility PROFIT. The merged SRD patterns for the four samples have been provided as Supplemental data.

Pattern indexing and space group checks were conducted with the HSP program, and Rietveld computations were performed with HSP and also parallel Rietveld calculations conducted with the Bruker Topas (Version 5) program. The CIF file used to model the $CuSO_4$. $5H_2O$ crystal structure was taken from ICSD-60059.

IV. RESULTS AND DISCUSSION

A. Moolooite SRD patterns

Figure 5 shows moolooite SRD patterns A and B. It is evident from the plots that the space group decribes the diffraction

https://doi.org/10.1017/S0885715619000101 Published online by Cambridge University Press

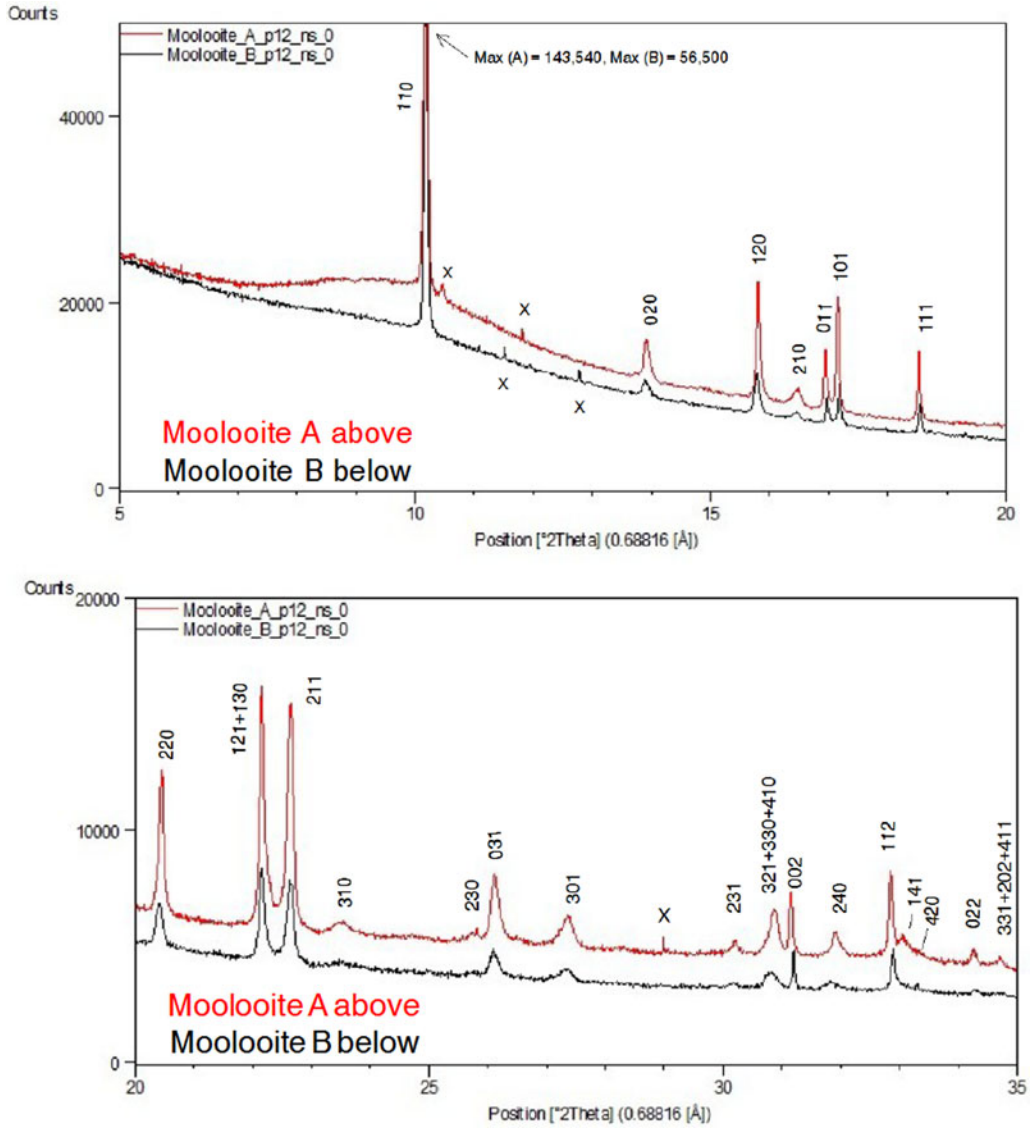

Figure 5. (Color Online) SRD patterns for the Moolooite C7 material. Moolooite A is from a turquoise coloured section of the capillary; and Moolooite B is from the grey section. $\lambda = 0.68816$ Å. Line *hkl* indices for space group *Pnnm* – see Table I. *x*: contaminant lines (see Table II).

line positions very well and that the indexing is in accord with that by Clarke and Williams (1986) for DS data. There is no evidence in the SRD patterns for (i) supercell lines reported by Clarke and Williams (see Table I) or (ii) for additional lines for the β-Cu oxalate polymorph which is also described as the MDO_1 polytype – see Figure 4. Accordingly, it is confirmed that the moolooite specimens examined are described by the FDSF superposition structure. Comparison of Patterns A and B showed that there are no pattern differences evident which might point to crystallographic differences. The overall intensities of the Bragg peaks for pattern A are approximately 3× more intense than those for Pattern B on which basis Pattern A was used for the subsequent crystallographic work having effectively a substantially greater diffracting volume. Both patterns have impurity features according to the identifications provided in Table II.

Table I gives an analysis of the moolooite SRD data set in sufficient detail to provide data for natural moolooite in the ICDD-PDF database. The attachment also compares the SRD data with the DS data published by Clarke and Williams (1986). The following observations are made from the comparison. Overall, there is consistency between the SRD and DS data sets with the exception of the two weak, "diffuse" lines reported by Clarke & Williams which appear to correspond to the most intense non-family MDO_1 polytype lines. As expected, the SRD set has added substantial additional information to that from the laboratory DS set – notably by detecting additional lines, and importantly by providing line width estimates. The additional 13 SRD lines are all very weak lines which would be below the laboratory DS detection limit.

The moolooite space group was determined with great caution in view of the similarities in patterns for the orthorhombic and monoclinic polymorphs. The HSP search program was used for *ab-initio* indexing with the algorithms: DICVOL04 (Boltif and Louer algorithm) and TREOR90 (Werner algorithm). The same solution was obtained for all calculations using 29 fully-resolved lines. The SRD orthorhombic fit from indexing after least squares fitting, assuming *Pnnm*, gave reasonable agreement between the measured and

https://doi.org/10.1017/S0885715619000101 Published online by Cambridge University Press

TABLE I. Moolooite SRD data (Pattern A) compared with Debye-Scherrer XRD data from Clarke and Williams (1986).

	SRD Data (This study) 0.68816 Å										Debye-Scherrer Camera (Clarke and Williams, 1986) – Co Tube. Visual intensities			
#	$2\theta_{obs}$	$2\theta_{cal}$	$\Delta 2\theta$	d_{obs}	d_{cal}	I_{obs}	FWHM	h	k	l	d_{obs}	d_{cal}	I_{obs}	Comments
											4.61d	–	<5	Described as "super-cell reflection" – Footnote 2
1	10.1816	10.1815	0.0001	3.8776	3.8777	123 239	0.049	1	1	0	3.88	3.881	100	
											3.54d	–	<5	Described as "super-cell reflection" – Footnote 2
2	13.9147	13.9166	−0.0019	2.8406	2.8402	4276	0.106	0	2	0	2.83	2.817	12	
3	15.8017	15.7958	0.0059	2.5031	2.5041	12 664	0.072	1	2	0	2.50	2.493	30	
4	16.4578	16.4585	−0.0007	2.4040	2.4039	1748	0.153	2	1	0	2.41b	2.418	10	
5	16.9383	16.9389	−0.0006	2.3363	2.3362	6409	0.056	0	1	1	2.33	2.331	18	
6	17.1485	17.1482	0.0003	2.3079	2.3079	10 309	0.046	1	0	1	2.31	2.309	25	
7	18.5292	18.5211	0.0000	2.1382	2.1382	7517	0.044	1	1	1	2.14	2.137	20	
8	20.4499	20.4446	0.0053	1.9383	1.9388	5944	0.090	2	2	0	1.938	1.940	18	
9	22.1537	22.1512	0.0025	1.7909	1.7911	9968	0.088	1	2	1	1.787	1.786	25	Line overlap - minor influence
	22.2544	22.2491	0.0053	1.7829	1.7833	3333		1	3	0		1.784		Line overlap – RTV inferred
10	22.6406	22.6344	0.0062	1.7529	1.7534	9635	0.115	2	1	1	1.753	1.758	30	
11	23.4976	23.5115	−0.0139	1.6898	1.6888	464	0.280	3	1	0	1.689	1.701	<5	Broad SRD and DS peak
12	25.7964	25.7999	−0.0035	1.5414	1.5412	419	0.060	2	3	0				
13	26.1115	26.1153	−0.0038	1.5232	1.5229	2947	0.155	0	3	1	1.518b	1.514	15	
14	27.3547	27.3431	0.0016	1.4558	1.4552	1322	0.228	3	0	1	1.459b	1.464	10	
15	30.2014	30.2001	0.0013	1.3208	1.3208	511	0.102	2	3	1				
		30.8045			1.2955			3	2	1		1.299		
16	30.8682	30.8767		1.2929	1.2966	1965	0.190	3	3	0	1.293b	1.294	10	Line overlap
		30.8943			1.2918			4	1	0				
17	31.1486	31.1498	−0.0012	1.2816	1.2815	2836	0.064	0	0	2	1.279	1.280	12	
18	31.9110	31.9022	0.0088	1.2517	1.2520	1002	0.139	2	4	0	1.247b	1.246	<5	
19	32.8480	32.8525	−0.0045	1.2169	1.2168	3635	0.072	1	1	2	1.216	1.216	15	
20	33.0557	33.0565	−0.0008	1.2095	1.2095	773	0.176	1	4	1				
21	33.2528	33.2693	−0.0165	1.2025	1.2020	588	0.101	4	2	0				
22	34.2514	34.2688	−0.0114	1.1685	1.1681	750	0.103	0	2	2	1.163	1.165	<5	
		34.6915			1.1541			3	3	1		1.155		
23	34.6948	34.6963		1.1540	1.1539	444	0.116	2	0	2	1.154	1.155	<5	Line overlap
		34.7074			1.1536			4	1	1				
24	35.1077	35.1094	−0.0017	1.1408	1.1408	444	0.085	1	2	2	1.138	1.139	<5	
25	37.5473	37.5494	−0.0021	1.0689	1.0691	1018	0.092	2	2	2	1.069	1.068	10	
26	38.6153	31.6144	0.0009	1.0406	1.0407	408	0.173	1	3	2	1.038	1.038	<5	
27	39.3914	39.3943	−0.0029	1.0209	1.0209	250	0.290	3	1	2				
28	40.2384	40.2383	0.0001	1.0003	1.0003	290	0.240	4	3	1				
		41.5789			0.9694			4	4	0				
29	41.6624	41.6807		0.9675	0.9672	340	0.260	2	5	1				Line overlap
		41.7215			0.9663			5	1	1				
30	42.1944	42.1951	−0.0007	0.9559	0.9559	300	0.140	3	5	0				
31	44.4346	44.4312		0.9100	0.9100	487	0.125	3	3	2	0.910	0.913	5	Line overlap
		44.4441			0.9098			4	1	2				
32	45.1813	45.1853		0.8957	0.8956	303	0.153	3	5	1				Line overlap
		45.1891			0.8956			2	4	2				
		48.0679			0.8448			0	1	3				
		48.0830			0.8446			6	2	0				Line overlap
33	48.1302	48.1502		0.8438	0.8435	256	0.166	1	0	3				

[1)]Contaminant lines omitted – see Table II. d-spacings calculated for space group Pnnm lines with Rietveld unit-cell parameters $a = 5.3064$, $b = 5.6804$, $c = 2.5630$ Å.
[2)]The diffuse 4.61 and 3.54 Å lines from Clarke & Williams Debye-Scherrer data may be MDO_1 polytype reflections, 10–1 and 11–1, respectively.
[3)]Smith-Snyder figure-of-merit for indexing of SRD data (excluding overlapping lines): First 26 resolved lines to $2\theta = 42.19°$, $d = 0.956$ Å: $< |\triangle(2\theta)| > = 0.0042°$, $F_{26} = 87$ (0.0042, 37).

calculated line positions, with a Smith-Snyder figure-of-merit $F_{26} = 87$ (0.0081, 37). From Rietveld analysis, the optimised unit-cell parameters gave improved agreement which reflects the excellent quality of the SRD measurements: $F_{26} = 167$ (0.0042, 37). It is noted also that the best monoclinic fit to the Pattern A data assuming the monoclinic space group $P2_1/n$ was poor according to expectations for SRD data: $F_{29} = 4.4$ (0.023, 296) which indicates that the moolooite material reported here cannot be described as monoclinic. The final set of moolooite unit-cell parameters – see Table I – was

https://doi.org/10.1017/S0885715619000101 Published online by Cambridge University Press

TABLE II. Impurity phase identifications for SRD mooloolite patterns A and B, and for the synthetic Cu oxalate pattern CSIRO-SYN.

2θ (°)	d-spacing (Å)	Peak height (counts) >1000	Peak height (rel %)	FWHM (°)	Identification from PDF
Mooloolite pattern A					
10.467	3.772	1331	1.0	0.039	Middlebackite[a], 3.769 Å, I_{100}
11.811	3.344	1379	1.1	0.010	Quartz, 00-46-1045: 3.343 Å, I_{100}
Mooloolite pattern B					
11.497	3.435	1120	3.0	0.022	Barite, 01-83-3078, 3.444 Å, I_{100}
12.760	3.096	1505	4.1	0.025	Barite, 3.103 Å, I_{100}
Synthetic Cu oxalate CSIRO-SYN. Impurity lines due to $CuSO_4$. $5H_2O$, 00-11-0646					
6.880	5.734	1861	0.7	0.015	Int = 35, d = 5.730
7.197	5.482	2376	0.8	0.015	55,5.480
8.354	4.724	4450	1.6	0.013	100,4.730
8.456	4.667	1146	0.4	0.014	20,4.660
9.899	3.988	3173	1.1	0.011	60,3.990
10.649	3.708	3711	1.3	0.014	85,3.710
11.438	3.453	1181	0.4	0.010	17,3.450
11.953	3.304	1735	0.6	0.012	60,3.300
14.167	2.790	2206	0.5	0.010	20,2.788
14.368	2.751	2358	0.8	0.010	50,2.749
14.853	2.664	1143	0.4	0.011	40,2.662

[a]Middlebackite, $Cu_2C_2O_4(OH)_2$: new copper oxalate mineral (Elliott, 2016 and 2018; Clarke and O'Connor In progress and O'Connor *et al*., In progress).

$a = 5.3064(2)$, $b = 5.6804(2)$, $c = 2.5630(1)$ Å. Space group possibilities were examined using HSP which identified *Pnnm* (#58) as the best possible space group choice according to the systematic absence conditions: $h0l$, $h + l = 2n$; $0kl$, $k + l = 2n$; $h00$, $h = 2n$; $0k0$, $k = 2n$; $00l$, $l = 2n$. However it is noted for the axial reflections that (i) $h00$ reflections were not detected, and (ii) only 020 was measured for $0k0$ and only 002 for $00l$.

B. Synthesised Cu oxalate SRD patterns

Figure 6 provides a comparison of the SRD patterns for the two synthesised Cu oxalate patterns. The following comments are made on the data.

- The two patterns both show clear evidence of the presence of additional "non-family" reflections expected for the MDO_1 polytype, as illustrated in Figure 4. In particular, CSIRO-SYN shows the broad non-family (NF) lines 10–1, 11–1, 101 and 111 and the overlapping line triplet 121/22–1/30–1, none of which is observed for mooloolite.
- The pattern for GCL-SYN is poorly defined relative to that for CSIRO-SYN which points to this sample having substantially reduced crystallinity, presumably because of the differences in the conditions under which the two synthetics were precipitated.
- The CSIRO-SYN pattern includes a sub-set of contaminant lines, all being because of a slight excess of $CuSO_4$. $5H_2O$ reagent in the synthesis – see Table II.

Table III gives the line-by-line analysis of the CSIRO-SYN data following the indexing procedure. Pattern indexing and space group determination were conducted as for the mooloolite pattern. A set of 20 lines which appeared to be free of peak overlap and for which the peak intensity exceeded 1000 units was selected for indexing. This included four reflections thought to be MDO_1 polytype reflections: 10–1, 11–1, 101 and 111 (see Figure 6). The DICVOL04 and TREOR 90 programs each gave the same solution: (i) monoclinic fit, with space group $P2_1/n$; (ii) least squares optimised cell parameters: $a = 5.957(7)$, $b = 5.611(5)$, $c = 5.133(7)$ Å; $\beta = 115.16(2)°$; (iii) measured-calculated line fits from indexing: $F_{20} = 2.9$ (0.078, 51). The indexing data fit is well outside the level of agreement expected for SRD data. In particular, there are lines for which the value of $|\Delta(2\theta)|$ exceeds 0.1°: MDO_1 lines 11–1 (0.13°) and 101 (−0.29°), and family lines 310 (0.31°), 40–2 (0.15°), 20–4 (0.11°), 11–4 (0.15°), 004 (0.18°) and 024 (0.18°). The large difference for 310 is not explained. The systematic absences for the SRD data indicate space group $P2_1/n$: $h0l$, $h + l = 2n$; $h00$, $h = 2n$; $0k0$, $k = 2n$; $00l$, $l = 2n$. However for the axial reflections (i) $h00$ reflections were not detected, and (ii) only 020 was observed for $0k0$.

C. Comparison of SRD patterns for mooloolite and synthesised Cu oxalate specimens

Figure 7 compares the mooloolite and CSIRO-SYN synthetic patterns. This underlines the comments of Schmittler (1968) that sample-sample line position differences may be observed depending on the synthesis conditions. The analysis of line position differences in Table III shows that the differences in line positions range from −0.221 to +0.255°, with the average difference magnitude being 0.075°. These large differences indicate the need to develop a set of suitable SRD patterns for a suite of synthetic Cu oxalates so that these may be characterised in greater detail.

D. Crystal data for mooloolite and synthesised Cu oxalate specimens: water content

Table IV summarises the crystal data for the mooloolite and synthetic Cu oxalate from this study and compares these with data from the literature. With reference to water content, Figure 8 shows the water-content calibration plots re-constructed from Schmittler (1968) who reported pyncnometry data for samples A, B, and F from that study. The Schmittler plots show trends in the a- and b-parameters for

https://doi.org/10.1017/S0885715619000101 Published online by Cambridge University Press

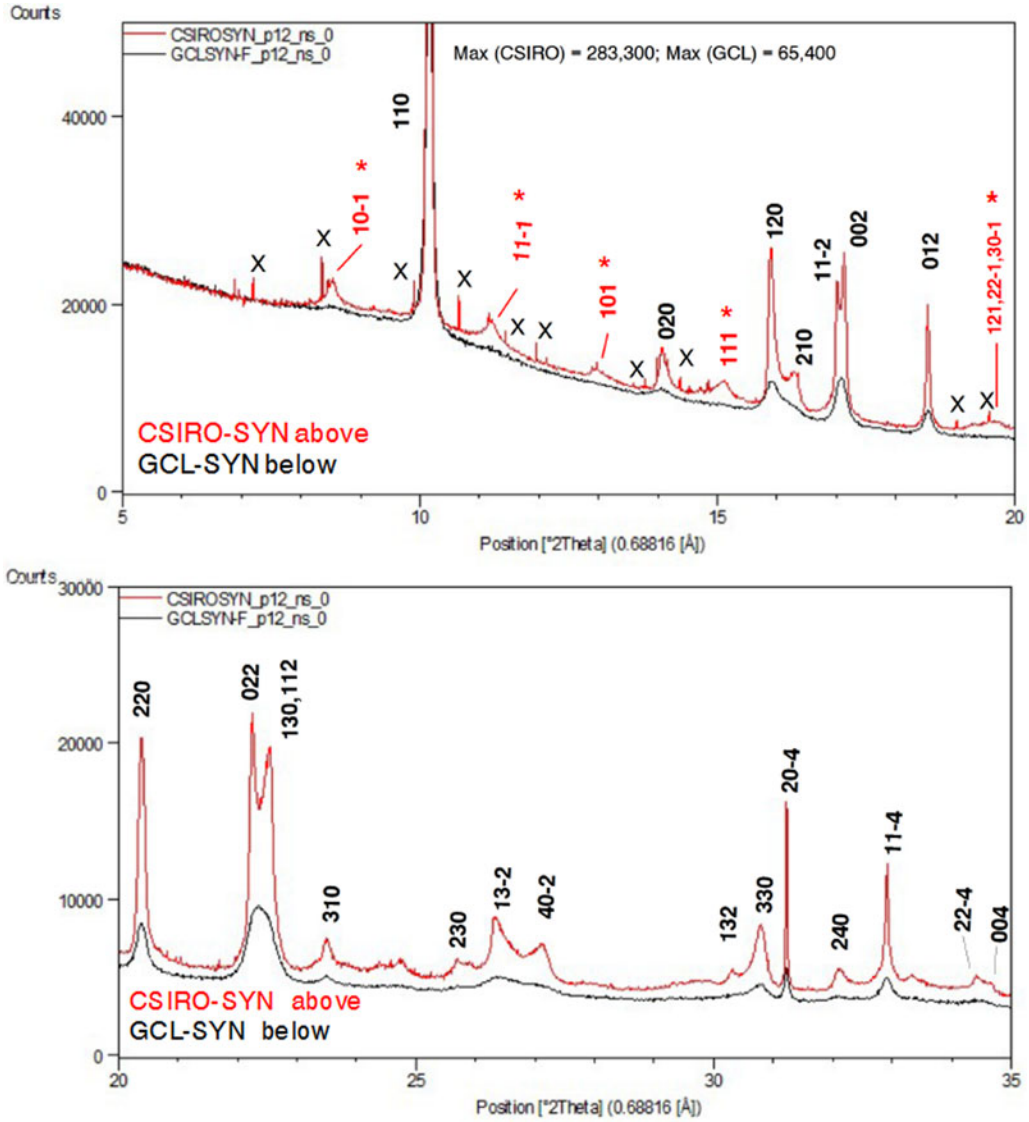

Figure 6. (Color online) SRD patterns for the synthetic Cu oxalate samples: CSIRO-SYN and GCL-SYN-F. $\lambda = 0.688161$ Å. Line *hkl* indices for space group $P2_1/n$ – see Table III. Indices in red (marked with asterisk) in (a) are MDO_1 polytype NF lines not observed for the natural moolooite material.

orthorhombic and monoclinic cells, with the latter being expressed for the equivalent pseudo-orthorhombic cell. The Schmittler linear relations in Figure 8 are –

$$a = 5.419 - 0.108\,n\text{Å}$$

$$b = 5.552 + 0.139\,n\text{Å}$$

where n represents the water content. $n H_2O$. The estimates of water content from Figure 8 for the samples considered in this SRD study indicate that for n in CuC_2O_4. nH_2O the value for Moolooite A was $n \approx 1.0$, whereas the value for the CSIRO-SYN sample was much smaller, $n \approx 0.3$. Overall the data points in Figure 8 indicate that the three natural samples have higher water content than the synthetics. This strengthens speculation from the literature that the level of zeolitic water in moolooite appears to depend on the conditions under which the sample forms – notably on the time taken for crystallisation to occur which is likely to be much longer in the natural environment.

E. Line broadening effects in the SRD data – microstrain and ordered domain sizes

The moolooite SRD lines all show substantial specimen broadening (ranging from *ca.* 0.03° to about 0.27°, noting that the instrument width is only *ca.* 0.015° (see Table I). Figure 9 shows the line width FWHM values (instrument corrected) vs. 2θ. Only strong lines (peak intensity >1000) and with minimal line overlap are included in the plot. It is evident that the moolooite lines all show specimen broadening (up to about 0.15°) pointing to microstrain and/or crystallite domain size broadening, and also that the broadening effects are anisotropic. The anisotropic broadening character resembles that for the synthetic copper oxalates reported by Christensen *et al.* (2014).

The Williamson-Hall plot for the *hk*0 reflections was used to obtain indicative information for strain and size notwithstanding the obvious anisotropic nature of the broadening. The intercept of the plot provides a crystallite size estimate of *ca.* 200 nm, and from the gradient a substantial microstrain estimate of 0.10%. The broadening is dominated by microstrain.

https://doi.org/10.1017/S0885715619000101 Published online by Cambridge University Press

TABLE III. Synthetic Cu Oxalate SRD data (CSIRO-SYN) compared with Mooloolite SRD data.

Synthetic Cu Oxalate (CSIRO-SYN) 0.68816 Å											Mooloolite SRD Data						
#	$2\theta_{obs}$	$2\theta_{cal}$	$\Delta 2\theta$	d_{obs}	d_{cal}	I_{obs}	FWHM	h	k	l	$2\theta_{obs}$	$\Delta 2\theta$ (mool -syn)	I_{obs}	h	k	l	Comments
1	8.5304	8.5364	−0.0060	4.6264	4.6232	2626	0.140	1	0	−1							MDO_1 polytype NF reflection
2	10.1584	10.1548	0.0036	3.8865	3.8878	282698	0.063	1	1	0	10.1815	0.023	123 239	1	1	0	
3	11.1934	11.0676	0.1258	3.5281	3.5681	1965	0.130	1	1	−1							MDO_1 polytype NF reflection
4	13.0940	13.3812	−0.2872	3.0178	2.9533	900	0.210	1	0	1							MDO_1 polytype NF reflection
5	14.0674	14.0891	−0.0217	2.8099	2.8056	3862	0.112	0	2	0	13.9147	−0.153	4276	0	2	0	
6	15.1064	15.1310	−0.0246	2.6176	2.6134	1340	0.136	1	1	1							MDO1 polytype NF reflection
7	15.8944	15.8932	0.0012	2.4886	2.4888	16 365	0.107	1	2	0	15.8017	−0.099	12 664	1	2	0	
8	16.2884	16.2805	0.0079	2.4288	2.4300	3648	0.160	2	1	0	16.4578	0.178	1748	2	1	0	
9	17.0094	16.9556	0.0538	2.3266	2.3339	13 694	0.190	1	1	−2	16.9389	−0.070	6409	0	1	1	
10	17.1264	17.0350	0.0914	2.3108	2.3231	16 971	0.089	0	0	2	17.1485	0.022	10 309	1	0	1	
11	18.5344	18.4490	0.0854	2.1366	2.1464	12 743	0.055	0	1	2	18.5292	−0.005	7517	1	1	1	
12	19.6714	19.4779		2.0142	2.0341	700	0.40	1	2	1							MDO_1 polytype NF reflection
12A		19.5344			2.0282			2	2	−1							Triplet
12B		19.9763			1.9838			3	0	−1							
13	20.3864	20.3905	−0.0041	1.9443	1.9439	13 323	0.110	2	2	0	20.4446	0.052	5944	2	2	0	
14	22.2494	22.1736	0.0758	1.7833	1.7893	15 702	0.118	0	2	2	22.1537	−0.096	9968	1	2	1	
15	22.5394	22.4562		1.7607	1.7671	13 640	0.132	1	3	0	22.2544		3333	1	3	0	Line overlap
15A		22.4232			1.7697			1	1	2	22.6406	0.1012	9635	2	1	1	
16	23.5024	23.1939	0.3085	1.6895	1.7116	1745	0.117	3	1	0	23.4976	−0.005	464	3	1	0	
17	25.7964	25.8764	−0.0800	1.5414	1.5368	419	0.045	2	3	0	25.7999	0.004	419	2	3	0	
18	26.3364	26.3154	0.0210	1.5104	1.5116	2664	0.140	1	3	−2	26.1153	−0.221	2947	0	3	1	
19	27.0994	26.9493	0.1501	1.4686	1.4766	1136	0.200	4	0	−2	27.3547	0.255	1322	3	0	1	Reflection
20	30.3064	30.2053	0.1011	1.3163	1.3206	781	0.140	1	3	2	30.2001	−0.106	511	2	3	1	
21	30.7864	30.7939	−0.0075	1.2963	1.2959	3624	0.200	3	3	0	30.8767	0.090	1965	3	3	0	
22	31.2174	31.1069	0.1105	1.2788	1.2832	11 841	0.027	2	0	−4	31.1498	−0.068	2836	0	0	2	
23	32.1024	32.1029	−0.0005	1.2444	1.2444	1030	0.136	2	4	0	31.9022	−0.200	1002	2	4	0	
24	32.9054	32.7563	0.1491	1.2149	1.2202	7388	0.072	1	1	−4	32.8525	−0.053	3635	1	1	2	
25	34.4044	34.2975	0.1069	1.1634	1.1670	746	0.094	2	2	−4	34.2688	−0.136	750	0	2	2	
26	34.6434	34.4617	0.1817	1.1557	1.1616	533	Broad	0	0	4	34.6963	0.053	444	2	0	2	
27	37.5794	37.3992	0.1802	1.0682	1.0732	1421	0.106	0	2	4	37.5494	−0.030	1018	2	2	2	
28	44.4144	44.4151	−0.0007	0.9104	0.9104	675	0.165	3	4	2	44.4312	0.017	487	3	3	2	
29	48.2104	48.0120		0.8425	0.8458	867	0.104	2	0	−6	48.1502	−0.060	256	1	0	3	Line overlap
29A		48.0147			0.8457			3	1	−6							

Contaminant lines omitted – see Table II. d-spacings calculated with unit-cell parameters $a = 5.957$, $b = 5.611$, $c = 5.133$ Å, $\beta = 115.16°$.
Smith-Snyder figure-of-merit for indexing of SRD data (excluding overlapping lines): First 20 resolved lines to $2\theta = 31.22°$, $d = 1.279$ Å: $< |\Delta(2\theta)| > = 0.078°$, $F_{20} = 2.9$ (0.078, 51).

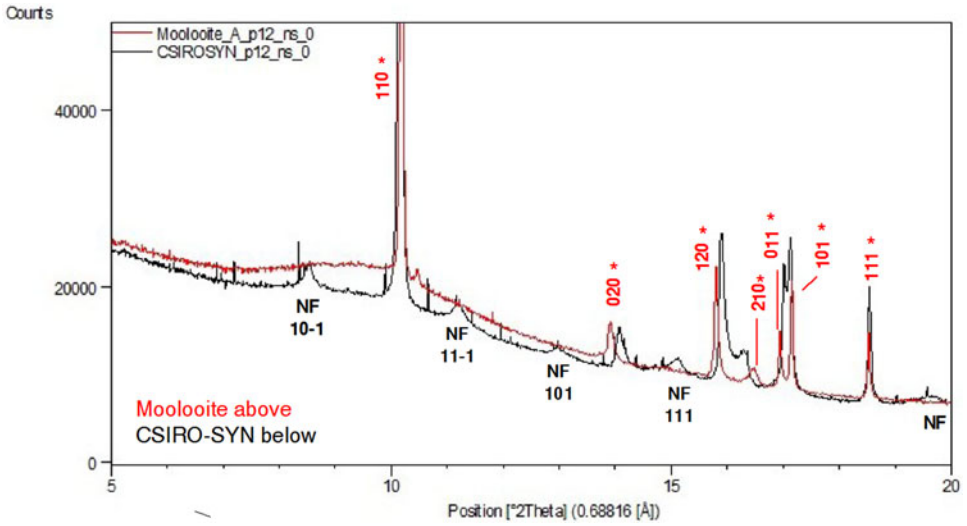

Figure 7. (Color Online) Comparison of SRD patterns of moolooite and synthetic CSIRO-SYN specimens. $\lambda = 0.688161$ Å. Moolooite line *hkl* indices in red (marked with asterisk) are for space group *Pnnm* – see Table I. NF = non-family lines for MDO_1 polytype.

F. Crystal structure analysis of natural and synthetic sample SRD data

1. Moolooite SRD pattern A

Rietveld structural model optimisation was conducted starting with atom coordinates from Schmittler (1968) transformed to space group *Pnnm*. The Rietveld calculations were run with two programs – *HighScore Plus* (Version 3.1) and *Topas* (Version 5) to check the reproducibility of the Rietveld calculations which proved to be excellent. The refinement involved fitting –

- Pattern background with a 15-term Chebyshev function
- Pseudo-Voigt and TCH-pV profile shape function types for the *HighScore Plus* and *Topas* computations, respectively.

The instrument 2θ-zero setting was fixed at the value determined with a calibration standard – see Table I.

TABLE IV. Comparison of unit-cell parameters from current study and water content estimates from the Schmittler (1968) calibrations – see Figure 8.

Orthorhombic symmetry				
Study	This study	Clarke and Williams (1986)	Chisholm *et al.* (1987)	
Specimen	Natural (Moolooite A)		Natural	Synthetic
Description	Mooloo Downs (Western Australia)		Lichens (Scandinavia)	Precipitation from solutions of $CuCl_2$ and oxalic acid
Space group	*Pnnm*			
a	5.3064 (2)	5.35	5.348–5.381	5.42 (1)
b	5.6804 (2)	5.63	5.625–5.639	5.58 (1)
c	2.5630 (1)	2.56	2.548–2.559	2.557 (2)
V_c	77.26 (1)	77.11	77.17 (average)	77.3 (3)
H_2O (*n*), Figure 8:	0.98 ± 0.06	0.60 ± 0.04	0.54 ± 0.04 (average)	0.1 ± 0.1
H_2O (*n*), element analysis:		0.44		

Monoclinic symmetry				
	This study		Christensen *et al.* (2014)	
Specimen	Synthetic (CSIRO-SYN): precipitation from solutions of $CuSO_4$. $5H_2O$ and oxalic acid		Synthetic: precipitation from solutions of $Cu(NO_3)_2$. $3H_2O$ and oxalic acid	
Space group	$P2_1/n$			
Unit-cell definition	Monoclinic cell	Pseudo-orthorhombic cell	Monoclinic cell	Pseudo-orthorhombic cell
a	5.957 (7)	5.392	5.9598 (1)	5.3872
b	5.611 (5)	5.611	5.6089 (1)	5.6089
c	5.133 (7)	2 × 2.566	5.1138 (1)	2 × 2.557
B	115.16 (2)	90	115.320 (1)	90
V_c	155.27	2 × 77.64	154.52	2 × 77.26
H_2O (*n*), Figure 8:		0.34±0.09		0.35±0.06
H_2O (*n*), element analysis:		0.04		

https://doi.org/10.1017/S0885715619000101 Published online by Cambridge University Press

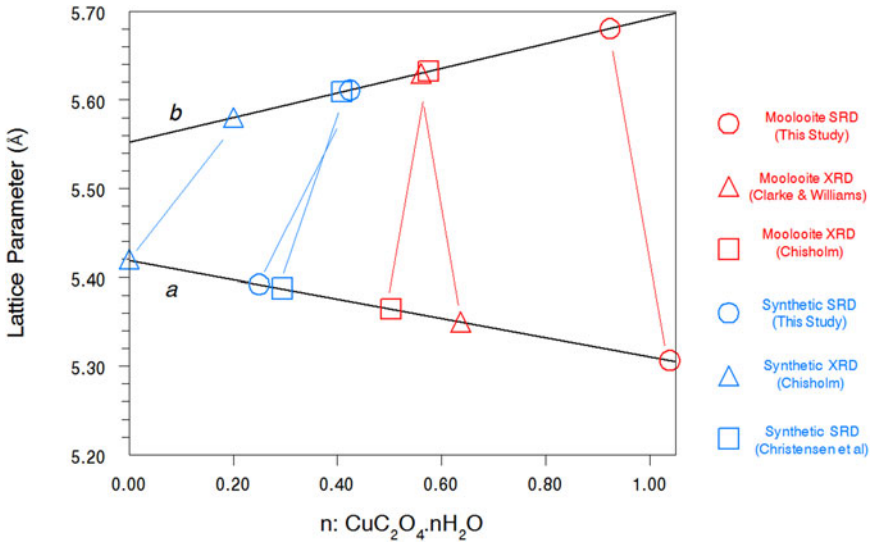

Figure 8. (Color online) Calibration plots *after* Schmittler (1968) based on unit cell parameters for orthorhombic and pseudo-orthorhombic data sets vs. measured value of water content: n in $CuC_2O_4.nH_2O$. Unit-cell parameters from present and other studies are shown with estimates of n from the Schmittler calibrations.

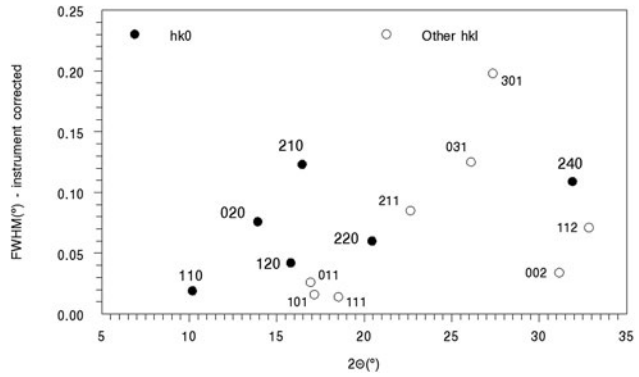

Figure 9. Line broadening for moolooite SRD pattern A. The most intense lines, with peak intensity >1,000, are shown in the plot.

The final parameter sets from the *Topas* program are given in Table V, and the Rietveld residual plot from program *Topas* is provided in Figure 10. The Rietveld calculations were more challenging than would be typically expected for a fully-ordered material. Importantly, we note from Table V that the Durbin-Watson statistic (Hill and Flack, 1987), DW, is 0.43 which indicates pronounced serial correlation between some parameters, in this case probably because of the planar groups and infinite linear molecules in the structure. Specifically, there were substantial correlations between the phase scale factor, the C and O atom positional parameters and the atom thermal parameters. The strong serial correlations between the atom positional parameters are shown in Table VI. The following substantial correlations are noted:

C(x/a): correlations with C(y/b) and O(z/c)

C(y/b): correlation with O(z/c).

Table VII provides the interatomic distances for the *Topas* atom parameter set, and compares these with values from the literature. We note that distances are probably acceptable taking into account the refinement correlations.

The residual plot indicates that all above-background Bragg peaks have been accounted for by the structural model, there being sound agreement between the calculated and measured lines other than the peak shape for some

TABLE V. Structural parameters from moolooite SRD Rietveld calculations.

	Schmittler (1968) model after RTV analysis	Schmittler (1968)
Global parameters:		
$2\theta_0$ (°)	0.0036	
Background	Chebyshev (15 terms)	
Phase parameters:		
Space group	*Pnnm*	
Scale	0.001538 (10)	
Unit-cell parameters (Å)		
a	5.3064 (2)	5.32–5.42
b	5.6804 (2)	5.55–5.66
c	2.5630 (1)	2.54–2.55
Vc(Å^3)	77.255 (4)	
Line profile	PV-TCHZ	
UCHZ	−0.62 (2)	
V	0.152 (6)	
W	−0.0083 (4)	
X	0.361 (13)	
Atom	Cu	
Wyckoff symbol	2a	
x/a	0	
y/b	0	
z/c	0	
B	1.0	
Atom	C	
Wyckoff	4 g	
x/a	0.1236 (14)	0.1174 (69)
y/b	0.0960 (10)	0.0968 (69)
z/c	0	0
B	1.0	
Atom	O	
Wyckoff symbol	8 h	
x/a	0.1995 (4)	0.1851 (39)
y/b	0.1534 (4)	0.1623 (32)
z/c	0.4712 (36)	0.502 (47)
B	1.0	
Figures-of-Merit:		
R_B	3.31	
Rwp [Rexp]	3.97 (1.33)	
χ^2	2.98	
DW	0.43	

https://doi.org/10.1017/S0885715619000101 Published online by Cambridge University Press

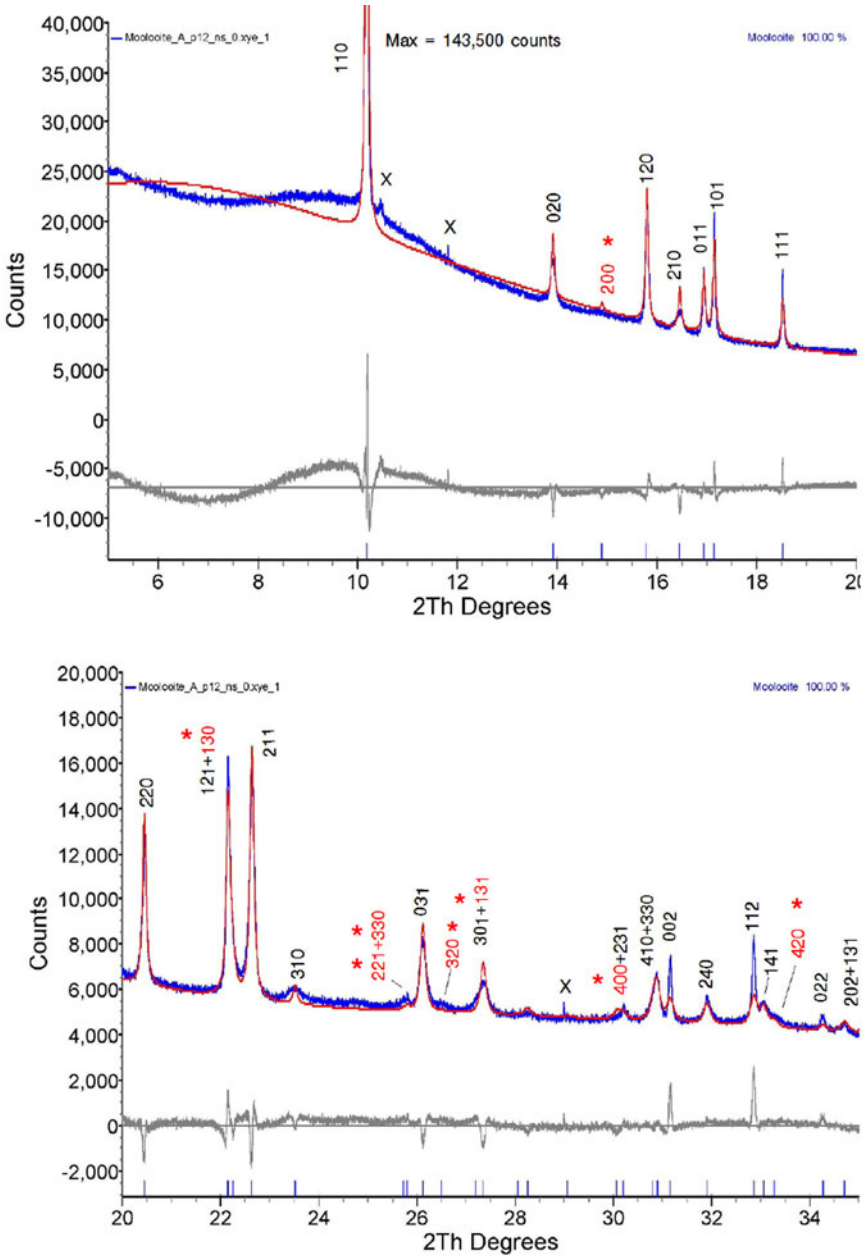

Figure 10. (color online) Rietveld difference residual plot for moolooite SRD pattern using the optimised structural model defined in Table V. Measured pattern in blue, calculated pattern in red. Symbol x = contaminant lines. *hkl* indices shown in red (marked with asterisk) are weak measured lines not listed in Table II of the Clarke & Williams study of moolooite DS data.

lines, noting that strain/size anisotropy was not factored into the refinement model. There is no indication of non-family lines for the MDO_1 polytype seen for the CSIRO-SYN specimen (see following subsection). The Rietveld residual plots were used to validate some line identities shown in Table I.

TABLE VI. Selected correlation coefficients between C and O atom positional parameters.

	C		O		
	x/a	*y/b*	*x/a*	*y/b*	*z/c*
C					
x/a	1.00	**0.42**	0.10	0.11	**−0.58**
y/b		1.00	0.08	−0.06	**−0.55**
O					
x/a			1.00	0.11	−0.11
y/b				1.00	−0.10
z/c					1.00

Schmittler moolooite orthorhombic model Rietveld optimised with SRD data – see Table V. Off-diagonal values greater than 0.40 are highlighted.

2. Synthetic copper oxalate structural model evaluations

The approach taken with respect to crystal structure for the synthetic material was to critically examine the structure models described in the literature, specifically –

- Structural polytypes according to OD theory as described by Fichtner-Schmittler (1979), noting especially the MDO_1 and MDO_2 polytypes – see discussion above, "Structural Models for Copper Oxalate from the Literature"
- The ordered structural model proposed by Kondrashev *et al.* (1985), described as the β-oxalate polymorph which may be also described as the MDO_1 polytype
- The disordered model from Christensen *et al.* (2014).

https://doi.org/10.1017/S0885715619000101 Published online by Cambridge University Press

TABLE VII. Interatomic distances (Å) for mooloite SRD Rietveld structural optimisation calculations.

Contact	Mooloite SRD (This Study)	Literature values			
		Cu Oxalate (Schmittler, 1968)	Cu Oxalate (Christensen *et al*., 2014)	Metal Oxalates – [chelating, $\eta^2(O_2C)_2$] (Int Tab Cryst, 1995)	Cu Carboxylates (O'Connor and Maslen, 1966)
Cu-O (intra-ribbon)	1.827 (3)–4 bonds	1.85	1.918 (8), 2.081 (7)	1.949	1.97
Cu-O (inter-ribbon)	2.535 (2)–2 bonds	2.54	Not reported		
C-O	1.314 (9)	1.37	1.26 (1), 1.27 (1)	1.224	1.25
C-C	1.705 (14)	1.66	1.576 (6)	1.546	1.52

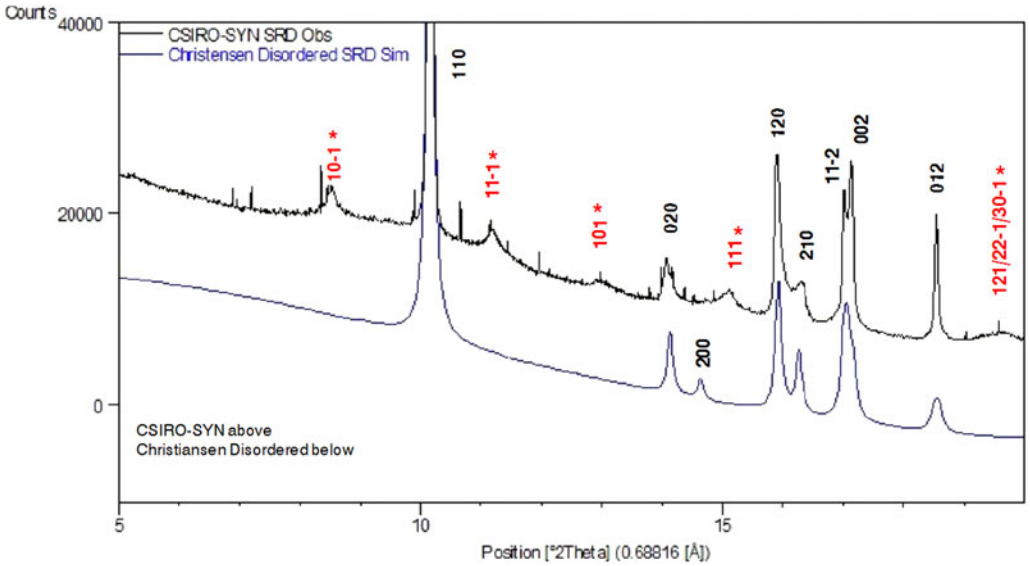

Figure 11. (Color online) Simulation testing of monoclinic structural models from Christensen *et al*. (2014). Comparison with the measured SRD pattern for CSIRO-SYN material. Line *hkl* indices for space group $P2_1/n$ – see Table III. Indices in red (marked with asterisk) are MDO_1 polytype NF lines not observed for the mooloite material. The very narrow lines are because of the $CuSO_4$. $5H_2O$ contaminant (*ca.* 3% by weight).

SRD pattern simulations were conducted for each of the models to test agreement with the measured SRD patterns. The comparisons showed (i) reasonable agreement between measured and simulated patterns for the Fichtner-Schmittler MDO_1 polytype; but (ii) less agreement for the Kondrashev *et al*. (1985) and Christensen *et al*. (2014) models. By way of example, Figure 11 shows a comparison of the Christensen *et al*. (2014) simulation with the measured SRD pattern for CSIRO-SYN, with the indexing for the measured pattern indicating the sound agreement for the Fichtner-Schmittler MDO1 structure. The Christensen *et al*. (2014) model produces the family lines for the MDO_1 model seen in the measured pattern but does not generate the measured non-family lines.

Taking the above observations into account, and the obvious dependence of line positions and intensities on synthesis conditions, it is evident that there is a need for a major systematic study on the way in which synthesis conditions influence the disordered character of Cu oxalates. It is noted that the results of Rietveld optimisations with the CSIRO-SYN pattern (not reported here) were inconclusive owing to model shortcomings.

V. CONCLUSION

The SRD study has extended the results of the earlier mooloite crystallographic study using Debye-Scherrer photographic data (Clarke and Williams, 1986). In particular, it has been confirmed that mooloite has a FDSF structure with the orthorhombic space group *Pnnm* first proposed for synthetic copper oxalates by Schmittler (1968). SRD data from two synthetic specimens has shown a closely-related monoclinic structure with space group $P2_1/n$. The subtle differences in SRD diffraction patterns for the two forms are attributed to differences in disorder according to interpretations by Fichtner-Schmittler (1979) using OD theory. It is evident from this study and earlier work that the monoclinic diffraction patterns show differences in peak position, breadth and intensity which are attributed to conditions under which the material was synthesised. This clearly complicates the identification of synthetics. The complexity is best described by seeing the orthorhombic form as fully disordered, whereas monoclinic synthetics are partially disordered. The best structural fit to the synthetic SRD data was obtained using the model proposed by Christensen *et al*. (2014) from another SRD study of synthetics in which there are two equally-

https://doi.org/10.1017/S0885715619000101 Published online by Cambridge University Press

weighted configurations which are offset by $c/2$ in space group $P2_1/n$. However, this model does not simulate some of the weak non-family peaks predicted by Fichtner-Schmittler for the MDO_1 polytype.

The question of the level and form of water in the materials has been considered with the approach followed by Schmittler (1968) using thermogravimetry and pycnometry, which points to the mooloite material examined in this study having the formula $CuC_2O_4.nH_2O$ where $n \approx 1.0$, It is postulated that the absence of water reported for some synthetic specimens may be attributed to the conditions under which synthetic samples have been synthesised. The conditions under which mooloite forms naturally appear to favour the take up of zeolitic water. Further work of the type conducted by Schmittler is required to determine the degree of zeolitic water in individual samples.

From indexing, new PDF data for both mooloite and one of the synthetic specimens have been proposed for inclusion in the ICDD-PDF database to assist the identification of natural and synthetic copper oxalate specimens. It will be important for the future releases of the database to include high-quality patterns for natural mooloite as well as synthetic Cu oxalates.

Supplementary material

The supplementary material for this article can be found at https://doi.org/10.1017/S0885715619000101.

Acknowledgements

The Australian Synchrotron is thanked for providing access to the Powder Diffraction Beamline, and also Curtin University and the ChemCentre for use of the additional instrumentation and software used in the study. M Bussell, formerly of CSIRO Division of Mineralogy, is acknowledged for preparing the CSIRO-SYN synthetic mooloite, R Hermann of the Department of Chemistry, Curtin University for element analysis (CHN) of synthetic mooloite and D Allen of MBS Environmental for advice on the chemical synthesis. P Elliott of The University of Adelaide is acknowledged for providing a pre-proof copy of the accepted article Elliott (2018).

Chisholm, J. E. and Jones, G. C. and Purvis O. W. (**1987**). "Hydrated copper oxalate, moolooite, in lichens," Mineral. Mag. **51**, 715–718.

Christensen, A. N., Lebech, B., Andersen, N. H., and Grivel, J-C. (**2014**). "The crystal structure of paramagnetic copper (II) oxalate (CuC_2O_4): formation and thermal decomposition of randomly-stacked anisotropic nano-sized crystallites," Dalton T. **43**, 16754–16768.

Clarke, R. M. and O'Connor, B. H. (**In progress**). "New mineralogical data for moolooite and middlebackite from Mooloo Downs, Western Australia," Mineral. Mag.

Clarke, R. M. and Williams, I. R. (**1986**). "Moolooite, a naturally occurring hydrated copper oxalate from Western Australia," Mineral. Mag. **50**, 295–298.

Elliott, P. (**2016**). "Middlebackite, IMA 2015-115," CNMNC Newsletter No 30, April 2016, page 411; Mineral. Mag. **80**, 407–413.

Elliott, P. (**2018**). "Middlebackite, a new Cu oxalate mineral from Iron Monarch, South Australia: description and crystal structure," Pre-proof accepted article, Mineral. Mag. DOI: 10.1180/mgm.2018.136.

Fichtner-Schmittler, H. (**1979**). "On some features of x-ray powder patterns of OD structures," Cryst. Res. Technol. **14**, 1079–1088.

Fichtner-Schmittler, H. (**1984**). "Comments on the structure of copper (II) oxalate: discussion of x-ray powder diffraction and EXAFS results as a basis for interpretation of magnetic properties," Cryst. Res. Technol. **19**, 1225–1230.

Frost, R. L., Erickson, K., and Weier, M. (**2004**). "Thermal treatment of moolooite – a high resolution thermogravimetric and hot stage Raman spectroscopic study," J. Therm. Anal. Calorim. **77**, 851–861.

Gleizes, A., Maury, F., and Galy, J. (**1980**). "Crystal structure and magnetism of sodium bis(oxalate)cuprate(II) dihydrate, $Na_2Cu(C_2O_4)_2.2H_2O$. A deductive proposal for the structure of copper oxalate, $CuC_2O_4.xH_2O$ ($0 \leq x < 1$)," Inorg. Chem. **19**, 2074–2078.

Hill, R. J. and Flack, H. D. (**1987**). "The use of the Durbin-Watson *d* statistic in Rietveld analysis," J. Appl. Crystallog. **20**, 356–361.

ICDD (**2016**). *PDF-4 + 2016 (Database)*, edited by S. Kabekkodo (International Centre for Diffraction Data, New Town Square, PA, USA).

International Tables for X-ray Crystallography (**1995**). *Vol C: Mathematical, Physical and Chemical Tables*, edited by A.J.C. Wilson (Kluwer Academic Publishers, Dordrecht), pp. 707–791.

Kondrashev, Y. D., Bogdanov, V. S., Golubev, S. N., and Pron, G. F. (**1985**). "Crystal structure of the ordered phase of zinc oxalate and the structure of anhydrous Fe^{2+}, Co^{2+}, Ni^{2+}, Cu^{2+} and Zn^{2+} oxalates," J. Struct. Chem. **26**, 90–93.

Michalowicz, A., Girerd, J. J., and Goulon, J. (**1979**). "EXAFS determination of the copper oxalate structure. Relation between structure and magnetic properties," Inorg. Chem. **18**, 3004–3010.

O'Connor, B. H. and Maslen, E. N. (**1966**). "The crystal structure of copper(II) succinate dihydrate," Acta Crystallogr. **20**, 824–835.

O'Connor, B. H., Clarke, R. M., and Kimpton, J. A. (**In progress**). "Synchrotron radiation study of middlebackite [$Cu_2C_2O_4(OH)_2$] using a mineral specimen from Mooloo Downs, Western Australia and chemically synthesized material," Powder Diffr.

Schmitt, B., Bronnimann, C, Eikenberry, E. F., Gozzo, F., Horrmann, C., Horisberger, R., and Patterson, B. (**2003**). "Mythen detector system," Nucl. Instrum. Methods Phys. Res., Sect. A **501**, 267–272.

Schmittler, H. (**1968**). "Structural principles of disordered copper(II) oxalate (CuC2O4. nH2O)," Monatsber. Deut. Akad. Wiss. Berlin **10**, 581–604.

Wu, W-Y and Zhai, L-X (**2007**). "Poly[diaqua-μ-oxalato-copper(II) monohydrate," Acta Crystallogr., Sect. E: Struct. Rep. Online, m249-m430.